# Clusters as Ligands. 6. Mixed-Metal Cluster Carboxylates of Titanium and Zirconium Derived from $(\eta^5\text{-}C_5H_5)M'(CO)_2Co_2(CO)_6(\mu_3\text{-}CCOOH)$, M′ = Mo, W

Hiroshi Shimomura, Xinjian Lei, Maoyu Shang, and Thomas P. Fehlner*

*Department of Chemistry and Biochemistry, University of Notre Dame, Notre Dame, Indiana 46556*

*Received September 23, 1997*[⊗]

The cluster acid $CpM'(CO)_2Co_2(CO)_6(\mu_3\text{-}CCOOH)$ (M′ = Mo, W; Cp = $\eta^5$-$C_5H_5$), **1**, has been synthesized in good yield from the protected $(CO)_9Co_3(\mu_3\text{-}CC(O)OR)$ cluster by metal fragment exchange followed by acid hydrolysis. The protonolysis of group 4 M(IV)$(OR)_4$ (M = Zr, Ti) organic alkoxides with this new cluster acid leads to trimetal cluster M(IV) alkoxycarboxylates. The products, which were isolated in good yield as crystalline substances and characterized spectroscopically as well as crystallographically, are $Zr_2(\mu\text{-}OH)_2\{\mu\text{-}CpMo(CO)_2Co_2(CO)_6(\mu_3\text{-}CCO_2)\}_2\{\eta^2\text{-}CpMo(CO)_2Co_2(CO)_6(\mu_3\text{-}CCO_2)\}_4$, **2**; $Ti_4(\mu_3\text{-}O)_4(OR)_2)_4\{\mu\text{-}CpM'(CO)_2Co_2(CO)_6(\mu_3\text{-}CCO_2)\}_4$, **3** (M′ = Mo, R = $CH(CH_2)_3$, **3a**; M′ = W, R = $CH(CH_2)_3$, **3b**; M′ = Mo, R = $C_2H_5$, **3c**; M′ = W, R = $C_2H_5$, **3d**). Direct comparison of this chemistry with that of $[(CO)_9Co_3(\mu_3\text{-}CCO_2)]^-$, which is of similar size, shows the importance of the electronic properties of the cluster substituent in the metal coordination chemistry of the carboxylate functionality. The exclusive binding of the proximal isomer of the cluster ligand (Cp ring adjacent to the capping carbon) relative to the more stable distal isomer (Cp ring positioned away from the capping carbon) provides definitive evidence for the existence of a cluster electronic effect in the coordination properties of the attached $[-CO_2]^-$ group. The significantly different chemistry of cluster vs organic ligands arises in part from this electronic effect.



## Introduction

In earlier work, we have demonstrated a simple strategy for the construction of cluster arrays.[1] A functionalized transition metal cluster, suitable for acting as a ligand toward cationic transition metal centers, is used to form cluster coordination complexes. Until now we have utilized the $[(CO)_9Co_3(\mu_3\text{-}C-)]$ cluster, functionalized with a $[-CO_2]^-$ group, to prepare a variety of cluster metal carboxylates.[2−8] The resulting novel compounds express the properties of the $[(CO)_9Co_3(\mu_3\text{-}C-)]$ cluster as a substituent as well as provide precursors for the synthesis of unusual heterogeneous catalysts.[9−11]

In principle, this approach to the construction of cluster arrays can be varied by (a) changing the metal cluster, (b) changing the functional group and, hence, the type of coordination chemistry, or (c) increasing the number of functional groups on the cluster. In the following paper, we report on the variation of the metal cluster by describing some chemistry of the cluster ligands $[CpM'(CO)_8(\mu_3\text{-}CCO_2)]^-$ (M′ = Mo, W; Cp = $\eta^5$-$C_5H_5$) in forming Ti and Zr alkoxy- or oxoalkoxycarboxylates. The reactions of this ligand with Ti and Zr alkoxides permits the direct comparison of its chemistry with that of $[(CO)_9Co_3(\mu_3\text{-}CCO_2)]^-$ described in the preceding paper[12] and provides additional insight on the roles of the metal cluster as a substituent.

## Experimental Section

**General.** All operations were conducted under a dinitrogen atmosphere using standard Schlenk techniques.[13] Solvents were distilled before use from drying agents under $N_2$ as follows: sodium benzophenone ketyl for hexane and tetrahydrofuran and $P_2O_5$ for $CH_2Cl_2$. $(CO)_9Co_3(\mu_3\text{-}CCO_2CH(CH_3)_2)$ was prepared according to the literature methods.[4,7,14,15] M$(OR)_4$ (M = Ti; R = $-CH_2CH_3$, $-CH(CH_3)_2$; M = Zr, R = $-CH(CH_3)_2$), $Mo(CO)_6$, and a 2 M THF solution of NaCp were used directly as received from Aldrich. FT-IR spectra were measured on a Nicolet 205 spectrometer. $^1$H NMR spectra were recorded on a 300 MHz Varian FT-NMR spectrometer. Residual protons of solvent were used as the reference for the $^1$H signals. UV−Vis spectra were recorded on a Varian Cary-3 UV−vis spectrophotometer. Elemental analyses were performed by M-H-W Laboratories, Phoenix, AZ.

**$CpMo(CO)_2Co_2(CO)_6(\mu_3\text{-}CCOOH)$, 1a.** $Mo(CO)_6$ (8.8 g, 33 mmol) and a 2 M THF solution of NaCp (17 mL, 34 mmol)

[⊗] Abstract published in *Advance ACS Abstracts,* November 15, 1997.

(1) Cen, W.; Haller, K. J.; Fehlner, T. P. *Inorg. Chem.* **1991**, *30*, 3120.
(2) Cen, W.; Lindenfeld, P.; Fehlner, T. P. *J. Am. Chem. Soc.* **1992**, *114*, 5451.
(3) Cen, W.; Haller, K. J.; Fehlner, T. P. *Organometallics* **1992**, *11*, 3499.
(4) Cen, W.; Haller, K. J.; Fehlner, T. P. *Inorg. Chem.* **1993**, *32*, 995.
(5) Lei, X.; Shang, M.; Patil, A.; Wolf, E. E.; Fehlner, T. P. *Inorg. Chem.* **1996**, *35*, 3217.
(6) Lei, X.; Shang, M.; Fehlner, T. P. *Organometallics* **1996**, *15*, 3779.
(7) Lei, X.; Shang, M.; Fehlner, T. P.; Werner, R.; Haase, W.; Hautot, D.; Long, G. J. *J. Organomet. Chem.* **1997**, in press.
(8) Calvo-Perez, V.; Fehlner, T. P.; Rheingold, A. L. *Inorg. Chem.* **1996**, *35*, 7289.
(9) Bañares, M. A.; Dauphin, L.; Calvo-Perez, V.; Fehlner, T. P.; Wolf, E. E. *J. Catal.* **1995**, *152*, 396.
(10) Bañares, M. A.; Dauphin, L.; Lei, X.; Cen, W.; Shang, M.; Wolf, E. E.; Fehlner, T. P. *Chem. Mater.* **1995**, *7*, 553.
(11) Bañares, M.; Patil, A. N.; Fehlner, T. P.; Wolf, E. E. *Catal. Lett.* **1995**, *34*, 251.
(12) Lei, X.; Shang, M.; Fehlner, T. P. *Organometallics* **1997**, *16*, 5289.
(13) Shriver, D. F.; Drezdzon, M. A. *The Manipulation of Air Sensitive Compounds,* 2nd ed.; Wiley-Interscience: New York, 1986.
(14) Seyferth, D.; Hallgren, J. E.; Hung, P. L. K. *J. Organomet. Chem.* **1973**, *50*, 265.
(15) Seyferth, D. *Adv. Organomet. Chem.* **1976**, *14*, 97.

S0276-7333(97)00838-8 CCC: $14.00 

were put into 250 mL of THF and refluxed for 12 h to yield a pale yellow solution. To this solution, 10 g (19 mmol) of $(CO)_9Co_3(\mu_3\text{-}CCO_2CH(CH_3)_2)$ was added and stirred for 24 h at room temperature and 1 h at 40 °C. The dark green solution formed was then evaporated to dryness to afford a green powder. The green powder was extracted with 300 mL of $CH_2Cl_2$. A reddish-brown solid was separated by filtration. The $CH_2Cl_2$ solution obtained was dried under vacuum. $C_2H_5OH$ (500 mL) was used to extract the solid. Filtration with a funnel layered with Celite gave rise to a dark green solution, which was again evaporated to dryness. The dark green solid was identified as $CpMo(CO)_2Co_2(CO)_6(\mu_3\text{-}CCO_2CH(CH_3)_2)$. FAB MS (NBA): obsd 602 with isotopic pattern corresponding to $Mo_1$; calcd for $MoCo_2C_{18}H_{12}O_{10}$ 602. $^1$H NMR ($CDCl_3$, 20 °C, $\delta$): 5.45 ($C_5H_5$, s, 5H), 5.17−5.08 (CH, 1H, septet, $J$ = 6 Hz), 1.33 ($CH_3$, 6H, d, $J$ = 6 Hz). It was then dissolved in 100 mL of concentrated sulfuric acid with vigorous stirring. After the mixture was stirred for 4 h, the solution was poured into 500 g of cracked ice and dark green solid was collected. Dark green microcrystals were produced by dissolving the dark green solid in 100 mL of $CH_2Cl_2$, which was filtered and evaporated to dryness. $CpMo(CO)_2Co_2(CO)_6(\mu_3\text{-}CCOOH)$ (5.2 g) was collected. The yield is 50% based on the amount of Co. FAB MS (NBA) obsd 560 with isotopic pattern corresponding to $Mo_1$; calcd for $MoCo_2C_{15}O_{10}H_6$ 560. $^1$H NMR ($CDCl_3$, 20 °C, $\delta$): 5.49 (s, 5 H). IR (KBr, cm$^{-1}$): 2081 (s), 2028 (vs), 2008 (vs), 2002 (s), 1988 (s), 1941 (v, sh), 1890 (m, sh), 1632 (m), 1256 (m), 827 (m), 719 (m), 707 (m), 511 (m). IR ($CH_2Cl_2$, cm$^{-1}$): 2090 (m), 2080 (m), 2053 (s), 2032 (s), 2011 (s), 1943 (w, br), 1893 (w, br), 1678 (w), 1632 (m). Anal. Calcd for $MoCo_2C_{15}H_6O_{10}$: C, 32.17; H, 1.08. Found: C, 32.59; H, 1.17.

**$CpW(CO)_2Co_2(CO)_6(\mu_3\text{-}CCOOH)$, 1b.** This cluster acid was prepared in a similar manner to **1a**. The yield is 20% based on the amount of Co. FAB MS (NBA): obsd 648 with isotopic pattern corresponding to $W_1$; calcd for $WCo_2C_{15}H_6O_{10}$ 648. $^1$H NMR ($CDCl_3$, 20 °C, $\delta$): 5.52 (s, 5 H). IR (KBr, cm$^{-1}$): 2081 (s), 2030 (vs), 2005 (vs), 1983 (s), 1891 (w, sh), 1630 (m), 1259 (m), 836 (m), 512 (m). IR ($CH_2Cl_2$, cm$^{-1}$): 2088 (m), 2080 (m), 2051 (s), 2037 (vs), 2027 (s), 2009 (s), 1960 (w, br), 1889 (m), 1679 (w), 1632 (m). Anal. Calcd for $WCo_2C_{15}H_6O_{10}$: C, 27.81; H, 0.93. Found: C, 26.57; H, 0.80.

**$CpW(CO)_2Co_2(CO)_6(\mu_3\text{-}CCOOC_2H_5)$, 1c.** This cluster ester was prepared as indicated in the procedure for **1a**. The yield is 20% based on the amount of Co. FAB MS (NBA): obsd 676 with isotopic pattern corresponding to $W_1$; calcd for $WCo_2C_{17}H_{10}O_{10}$ 676. IR (KBr, cm$^{-1}$): 2080 (m), 2040 (m, sh), 2020 (s), 1995 (s), 1968 (m), 1946 (w), 1920 (w, sh), 1670 (m), 1236 (m). IR ($CH_2Cl_2$, cm$^{-1}$ ): 2090 (m), 2080 (m), 2055 (m, sh), 2040 (m, sh), 2029 (s), 2008 (s), 1957 (w), 1930 (w, sh), 1884 (w), 1670 (w), 1227 (m). Anal. Calcd for $WCo_2C_{17}H_{10}O_{10}$: C, 30.21; H, 1.49. Found: C, 30.28; H, 1.29.

**$Zr_2(\mu\text{-}OH)_2\{\mu\text{-}CpMo(CO)_2Co_2(CO)_6(\mu_3\text{-}CCO_2)\}_2\{\eta^2\text{-}CpMo(CO)_2Co_2(CO)_6(\mu_3\text{-}CCO_2)\}_4$, 2.** $CpMo(CO)_2Co_2(CO)_{62}(\mu_3$-$CCO_2H)$ (0.4 mmol, 0.223 g) and $[Zr(OCH(CH_3)_2)_4\cdot HOCH(CH_3)_2]_2$ (0.1 mmol, 0.077 g) were put into a 100 mL Schlenk flask. This flask was evacuated and refilled with dinitrogen several times before 20 mL of THF was added to the flask via syringe with rapid stirring. The mixture was stirred at 50 °C overnight, and the solvent was removed *in vacuo*. The resulting dark greenish-brown solid was dissolved in THF and filtered through a 5 mm filter of Celite, and the THF was removed under vacuum. The solid obtained was washed with diethyl ether until the ether solution changed from dark green to colorless. The green ether solution contains unreacted cluster acid. Brown **2** (120 mg) is collected with a yield of 56% based on the amount of cluster acid used. The product is soluble in THF, slightly soluble in toluene and $CH_2Cl_2$, and insoluble in hexane or ether. It is sensitive to air and moisture, decomposing into unidentified light brown solids. Recrytallization from a solution of THF layered with hexane gave rise to X-ray quality crystals. $^1$H NMR ($C_6D_6$, 20 °C, $\delta$): 4.962 (s, 5 H). IR (KBr, cm$^{-1}$): 3110 (w), 2959 (w), 2929 (w), 2872 (w), 2860 (w), 2088 (v), 2048 (vs, sh), 2047 (vs, sh), 2023 (vs), 1942 (m), 1894 (m), 1640 (w, br), 1508 (w), 1421 (w, sh), 1396 (m), 1393 (w), 1345 (m), 1068 (w), 830 (w), 800 (w), 792 (w), 746 (w), 566 (w), 518 (m), 474 (w), 444 (m). IR (THF, cm$^{-1}$): 2088 (m), 2050 (m), 2025 (vs), 1942 (w, br), 1896 (w), 1640 (w, br), 1421 (w), 1400 (w), 1346 (w). Anal. Calcd for $Zr_2Mo_6Co_{12}C_{98}H_{48}O_{64}$: C, 31.69; H, 1.30. Found: C, 32.81; H, 1.26.

**$Ti_4(\mu_3\text{-}O)_4(OCH(CH_3)_2)_4\{\mu\text{-}CpMo(CO)_2Co_2(CO)_6(\mu_3\text{-}CCO_2)\}_4$, 3a.** $CpMo(CO)_2Co_2(CO)_6CCOOH$ (0.201 g, 0.359 mmol) was dissolved in 30 mL of distilled THF in a Schlenk flask. To this solution, 0.05 mL (0.048 g, 0.17 mmol) of $Ti(OCH(CH_3)_2)$ was added. The reaction mixture was stirred overnight (10 h) at room temperature, and the solvent was removed under vacuum. The brown powder obtained was dissolved in 15 mL of distilled $CH_2Cl_2$ and filtered. There was no residue. The filtered solution was concentrated to 10 mL and layered with 50 mL of $(CH_3)_2CHOH$. After the mixture was allowed to stand at −10 °C for several days, dark brown crystals formed and were collected by filtration. The yield is 50% based on the amount of Ti. $^1$H NMR ($CDCl_3$, 20 °C, $\delta$): 5.682, 5.671 (2 s in a 0.17:1 ratio, 20 H, Cp); 4.699 (sept, $J$ = 6 Hz, 4 H, ($CH(CH_3)_2$)), 1.241, 1.209 (2 d in a 0.12:1 ratio, $J$ = 6.3 Hz, 24 H, ($CH(CH_3)_2$)). IR (KBr, cm$^{-1}$): 2087 (s), 2048 (s), 2025 (vs) 1938 (m), 1891 (m), 1483 (w), 1460 (w), 1423 (w), 1376 (m), 1364 (m), 1342 (m), 1125 (m), 1008 (m), 713 (m). IR ($CH_2Cl_2$, cm$^{-1}$): 2087 (m), 2052 (m), 2028 (vs), 1942 (m, br), 1895 (m), 1428 (w), 1379 (w), 1364 (w), 1344 (m). Anal. Calcd for $Ti_4Mo_4Co_8C_{73}H_{50}O_{48}Cl_2$ ($CH_2Cl_2$ solvent of crystallization): C, 31.17; H, 1.79. Found: C, 32.32; H, 1.77.

**$Ti_4(\mu_3\text{-}O)_4(OCH(CH_3)_2)_4\{\mu\text{-}CpW(CO)_2Co_2(CO)_6(\mu_3\text{-}CCO_2)\}_4$, 3b.** The preparation procedure was similar to that of **3b**. The yield is 42% based on the amount of Ti. $^1$H NMR ($CDCl_3$, 20 °C, $\delta$): 5.762, 5.748 (2 s in a 0.20:1 ratio, 20 H, Cp), 4.701 (sept, $J$ = 6 Hz, 4 H, ($CH(CH_3)_2$)), 1.231, 1.209 (2 d in a 0.15:1 ratio, $J$ = 6.0 Hz, 24 H, ($CH(CH_3)_2$)). IR (KBr, cm$^{-1}$): 2086 (s), 2047 (s), 2024 (vs), 1934 (m), 1884 (m), 1450 (w), 1421 (w), 1384 (w, sh), 1364 (m), 1346 (m), 1125 (w), 1008 (m), 710 (m). IR ($C_6H_6$, cm$^{-1}$): 2086 (m), 2051 (s), 2026 (vs), 1938 (m, br), 1889 (m), 1421 (w), 1393 (w), 1364 (m), 1348 (m). Anal. Calcd for $Ti_4W_4Co_8C_{73}H_{50}O_{48}Cl_2$ ($CH_2Cl_2$ solvent of crystallization): C, 27.77; H, 1.37. Found: C, 27.60; H, 1.73.

**$Ti_4(\mu_3\text{-}O)_4(OCH_2CH_3)_4\{\mu\text{-}CpMo(CO)_2Co_2(CO)_6(\mu_3\text{-}CCO_2)\}_4$, 3c.** $CpMo(CO)_2Co_2(CO)_6(\mu_3$-$CCOOH)$ (0.8 mmol, 0.446 g) was dissolved in 20 mL of $CH_2Cl_2$. The mixture was stirred at room temperature for 10 min. Then 0.088 mL (0.4 mmol) of $Ti(OCH_2CH_3)_4$ was added to the solution. The reaction mixture was stirred at room temperature overnight. $CH_2Cl_2$ was removed under vaccum. The black microcrystals were extracted with 15 mL of THF to yield a brown solution, which was layered with hexane. The black crystals which appeared after 1 week were collected and washed with hexane. The crystals are slightly soluble in THF, toluene, and $CH_2Cl_2$ but insoluble in hexane. The yield is 50% based on the amount of Ti. $^1$H NMR ($CDCl_3$, 20 °C, $\delta$): 5.797, 5.784, 5.774, 5.769 (4 s in a 0.2:0.9:1:1 ratio, 20 H, Cp), 4.361, 4.356 (2 q in a 1:0.5 ratio, $J$ = 7 Hz, 8 H, ($CH_2CH_3$)), 1.214, 1.199, 1.193 (3 t in a 0.6:1:1 ratio, $J$ = 7 Hz, 12 H, ($CH_2CH_3$)). $^{13}$C {$^1$H} NMR (125.7 MHz, $CDCl_3$, 20 °C, $\delta$): 94.41, 94.38, 94.34, 94.33 (Cp, in a 0.3:0.8:1:1 ratio), 76.44 ($CH_2CH_3$), 29.70 ($CH_2CH_3$). IR (KBr, cm$^{-1}$): 2087 (s), 2047 (s, sh), 2025 (vs), 1937 (s), 1890 (m), 1655 (w, br), 1482 (w), 1460 (w), 1376 (m), 1363 (m), 1342 (s), 1119 (m), 1073 (m), 715 (m), 617 (m), 611 (m), 572 (s), 518 (s), 459 (m), 450 (m, sh), 448 (w, sh). IR ($CDCl_3$, 20 °C, cm$^{-1}$): 2088 (s), 2054 (s), 2030 (vs), 1941 (w), 1893 (m), 1484 (w), 1462 (w), 1423 (w), 1378 (w), 1364 (w), 1344 (m). Anal. Calcd for $Ti_4Mo_4Co_8O_{48}C_{68}H_{40}$: C, 27.01; H, 1.33. Found: C, 26.59; H, 1.27.

**$Ti_4(\mu_3\text{-}O)_4(OCH_2CH_3)_4\{\mu\text{-}CpW(CO)_2Co_2(CO)_6(\mu_3\text{-}CCO_2)\}_4$, 3d.** The preparation procedure was similar to that of **3c**. The compound is slightly soluble in THF, toluene, and $CH_2Cl_2$ but insoluble in hexane. The yield is 60% based on the amount of Ti. $^1$H NMR ($CDCl_3$, 20 °C, $\delta$): 5.748, 5.740, 5.736, 5.729, 5.723, 5.717 (6 s in a 0.3:0.5:0.8:1:1:0.3 ratio, 20

**Table 1. Crystallographic Data for $CpW(CO)_2Co_2(CO)_6(\mu_3\text{-}CCO_2CH_2CH_3)$, 1c**

| | |
|---|---|
| empirical formula | $C_{17}H_{10}Co_2O_{10}W$ |
| fw | 675.98 |
| cryst syst | triclinic |
| space group | $P\bar{1}$ |
| $a$ (Å) | 8.1160(8) |
| $b$ (Å) | 8.1166(5) |
| $c$ (Å) | 16.283(2) |
| α (deg) | 91.153(7) |
| $\beta$ (deg) | 98.032(9) |
| $\gamma$ (deg) | 106.844(7) |
| $V$ (Å$^3$) | 1014.4(2) |
| $Z$ | 2 |
| temperature (K) | 293(2) |
| $D_{calcd}$ (Mg/m$^3$) | 2.213 |
| abs coeff (mm$^{-1}$) | 7.444 |
| cryst size (mm) | 0.52 × 0.27 × 0.02 |
| no. of unique data | 3948 |
| no. of obsd data ($I > 2\sigma(I)$) | 3679 |
| no. of variables | 271 |
| final $R$ indices [$I > 3\sigma(I)$] | R1[a] = 0.02439 |
| | wR2[b] = 0.03600 |

[a] $R1 = \sum||F_o| - |F_c||/\sum|F_o|$. [b] $wR2 = [\sum w(F_o - F_c)^2/\sum(w|F_o|)^2]^{1/2}$.

H, Cp), 4.366, 4.361 (2 q in a 1:0.8 ratio, $J$ = 7 Hz, 8 H, ($CH_2$-$CH_3$)), 1.225, 1.211, 1.207, 1.205 (4 t in a 0.8:1:0.9:0.8 ratio, $J$ = 7 Hz, 12 H, ($CH_2CH_3$)). IR (KBr, cm$^{-1}$): 2086 (s), 2046 (s, sh), 2023 (vs), 1931 (s), 1881 (m), 1482 (w), 1459 (w), 1384 (w, sh), 1363 (m, sh), 1346 (s), 1118 (s), 1072 (s), 1008 (m), 926 (w), 854 (w, sh), 840 (m), 807 (w), 711 (s), 618 (s), 611 (s), 608 (s), 578 (s), 523 (s), 509 (s), 474 (m), 465 (m), 460 (m, sh), 445 (s), 406 (m). IR ($CDCl_3$, 20 °C, cm$^{-1}$): 2088 (s), 2053 (s), 2028 (vs), 1938 (w), 1884 (m), 1482 (w), 1460 (w), 1421 (w), 1389 (w), 1364 (w), 1348 (m). Anal. Calcd for $Ti_4W_4Co_8O_{48}C_{68}H_{40}$: C, 30.57; H, 1.51. Found: C, 30.80; H, 1.96.

**Structure Determinations. General.** The X-ray diffraction data were collected either on an Enraf-Nonius CAD4 diffractometer equipped with graphite-crystal-monochromated Mo Kα radiation at room temperature or an Enraf-Nonius FAST area-detector diffractometer at low temperature. In the former case, cell constants were obtained from least-squares refinement, using the setting angles of 25 reflections in the range 24° < 2$\theta$ < 36°. Lorentz and polarization corrections were applied to the data. An empirical absorption correction based on a series of $\psi$-scans was applied to the data. In the latter case, data were collected at 130 K with a Mo rotating anode source ($\lambda$ = 0.710 73 Å). The MADNES package was employed for cell constant determination, image measurement, and intensity data evaluation. The detailed procedure for small molecules using an area detector has been described elsewhere.[16] Each structure was solved by either the MULTAN direct method of the SDP package or the SHELXS-86 program followed by difference Fourier syntheses. Metal atoms were located from an $E$-map. The remaining atoms were found in succeeding difference Fourier syntheses. Preliminary least-squares refinement was performed with the SDP package, and further full-matrix least-squares refinements were carried out by using the SHELXL-93 program[17] based on $F^2$ for all reflections, except for **1c**. Crystal data are given in Tables 1 and 2. Specific details for each structure follow.

**$CpW(CO)_2Co_2(CO)_6(\mu_3\text{-}CC(O)OC_2H_5)$, 1c.** A brown plate-like crystal was mounted on a glass fiber in a random orientation. The structure was refined by full-matrix least-squares of the SDP package. Hydrogen atoms were located and added to the structure factor calculations, but their parameters were not refined. The final cycle of refinement converged to R1 = 0.02439 and R2 = 0.03600 for 3679 reflections with $I > 3\sigma(I)$. The highest peak in the final difference Fourier map was 1.04 e/Å$^3$, and the minimum negative peak was −0.99 e/Å$^3$.

**$Zr_2(\mu\text{-}OH)_2\{\mu\text{-}(CpMo(CO)_2Co_2(CO)_6(\mu_3\text{-}CCO_2)\}_2\{\eta^2\text{-}CpMo(CO)_2Co_2(CO)_6(\mu_3\text{-}CCO_2)\}_4\cdot 2THF$, 2·2THF.** Data were collected using an Enraf-Nonius FAST area-detector diffractometer at 130 K. Full-matrix least-squares refinements based on $F^2$ were employed for all reflections with bond length restraints for the ring atoms of the THF solvated molecules. After all non-hydrogen atoms were refined anisotropically, hydrogen atoms of the hydroxyl and cyclopentadienyl groups were located in an $E$-map, and their positional parameters were idealized with a riding model in the final refinement along with the rest of the hydrogen atoms calculated by the program. The refinement converged to a final value of R1 = 0.0683 for 10 449 reflections with $F_o^2 > 2\sigma(F_o^2)$ and wR2($F^2$) = 0.1694 for all data, and GOF = 1.074 (712 variables refined). The highest peak (near metal atom) in the final difference Fourier map was 1.910 e/Å$^3$, and the minimum negative peak was −1.083 e/Å$^3$.

**$Ti_4(\mu_3\text{-}O)_4(OCH(CH_3)_2)_4\{\mu\text{-}CpMo(CO)_2Co_2(CO)_6(\mu_3\text{-}CCO_2)\}_4\cdot CH_2Cl_2$, 3a·$CH_2Cl_2$.** A black polyhedron-like crystal was mounted on the top of a glass fiber, and data were collected with an Enraf-Nonius CAD4 diffractometer. The difference Fourier map indicated that one of the isopropoxy groups was disordered, and their site occupancy coefficients were included in the final least-squares refinement. All non-hydrogen atoms were refined with anisotropic thermal parameters, and hydrogen atoms were refined with a riding model and included in the final cycle, R1 = 0.0497 for 10 536 reflections with $F_o > 4\sigma(F_o)$, wR2($F^2$) = 0.1213 for 13 029 unique observed reflections, and GOF = 1.133 (1270 variables refined). The highest peak in the final difference Fourier map was 0.76 e/Å$^3$, and the lowest negative peak was −0.553 e/Å$^3$.

**$Ti_4(\mu_3\text{-}O)_4(OCH(CH_3)_2)_4\{\mu\text{-}CpW(CO)_2Co_2(CO)_6(\mu_3\text{-}CCO_2)\}_4\cdot CH_2Cl_2$, 3b·$CH_2Cl_2$.** A black polyhedron-like crystal was mounted on the top of a glass fiber, and data were collected with an Enraf-Nonius CAD4 diffractometer. All non-hydrogen atoms were refined with anisotropic thermal parameters, and hydrogen atoms were refined with a riding model and included in the final cycle, R1 = 0.0445 for 12 367 reflections with $F_o > 4\sigma(F_o)$, wR2($F^2$) = 0.1161 for 13 922 unique observed reflections, and GOF = 1.079 (1251 variables refined). The highest peak (near metal atom) in the final difference Fourier map was 1.234 e/Å$^3$, and the minimum negative peak was −0.554 e/Å$^3$.

**$Ti_4(\mu_3\text{-}O)_4(OCH_2CH_3)_4\{\mu\text{-}CpMo(CO)_2Co_2(CO)_6(\mu_3\text{-}CCO_2)\}_4$, 3c.** A black column-like crystal was mounted on the top of a glass fiber, and data were collected on a CAD4 diffractometer. All non-hydrogen atoms were refined with anisotropic thermal parameters, and hydrogen atoms were refined with a riding model and included in the final cycle, R1 = 0.0663 for 3166 reflections with $F_o > 4\sigma(F_o)$, wR2($F^2$) = 0.1864 for 3473 unique observed reflections, and GOF = 1.104 (298 variables refined). The highest peak in the final difference Fourier map was 1.631 e/Å$^3$ (near metal atom), and the minimum negative peak was −0.494 e/Å$^3$.

**$Ti_4(\mu_3\text{-}O)_4(OCH_2CH_3)_4\{\mu\text{-}CpW(CO)_2Co_2(CO)_6(\mu_3\text{-}CCO_2)\}_4$, 3d.** A black polyhedron-like crystal was mounted on the top of a glass fiber, and data were collected with an Enraf-Nonius CAD4 diffractometer. All non-hydrogen atoms were refined with anisotropic thermal parameters, and hydrogen atoms were refined with a riding model and included in the final cycle, R1 = 0.0305 for 3326 reflections with $F_o > 4\sigma(F_o)$, wR2($F^2$) = 0.0861 for 3457 unique observed reflections, and GOF = 1.075 (298 variables refined). The highest peak in the final difference Fourier map was 0.917 e/Å$^3$ (near metal atom), and the minimum negative peak was −0.419 e/Å$^3$.

## Results and Discussion

**Synthesis of the Cluster Ligand.** A cluster is of little value as a ligand if it cannot be prepared in good

(16) Scheidt, W. R.; Turowska-Tyrk, I. *Inorg. Chem.* **1994**, *33*, 1314.
(17) Sheldrick, G. M. *Siemens XRD*; Siemens, Inc.: Madison, WI, 1990.

**Table 2. Crystallographic Data for 2, 3a·$CH_2Cl_2$, 3b·$CH_2Cl_2$, 3c, and 3d**

| | **2** | **3a**·$CH_2Cl_2$ | **3b**·$CH_2Cl_2$ | **3c** | **3d** |
|---|---|---|---|---|---|
| empirical formula | $C_{98}H_{48}Co_{12}O_{48}Mo_6Zr_2$ | $C_{73}H_{50}Cl_2Co_8O_{48}Mo_4Ti_4$ | $C_{73}H_{50}Cl_2Co_8O_{48}Ti_4W_4$ | $C_{63}H_{40}Co_8O_{48}Mo_4Ti_4$ | $C_{68}H_{40}Co_8O_{48}Ti_4W_4$ |
| fw | 3714.60 | 2812.83 | 3164.47 | 2671.80 | 3023.44 |
| cryst syst | monoclinic | monoclinic | monoclinic | tetragonal | tetragonal |
| space group | *C*2/*c* | $P2_1$ | $P2_1$ | $I\bar{4}$ | $I\bar{4}$ |
| *a* (Å) | 25.147(3) | 14.872(2) | 14.863(3) | 16.642(2) | 16.6175(11) |
| *b* (Å) | 17.094(2) | 24.336(2) | 24.341(5) | 16.642(2) | 16.6175(11) |
| *c* (Å) | 31.675(3) | 14.921(2) | 14.953(2) | 18.010(4) | 17.970(3) |
| $\beta$ (deg) | 118.68(1) | 111.930(11) | 112.10(2) | | |
| *V* (Å$^3$) | 11 870(2) | 5009.3(11) | 5012(2) | 4987.8(14) | 4962.4(9) |
| *Z* | 4 | 2 | 2 | 2 | |
| temperature (K) | 130(2) | 293(2) | 293(2) | 293(2) | 293(2) |
| $D_{calcd}$ (Mg/m$^3$) | 2.079 | 1.865 | 2.097 | 1.779 | 2.023 |
| abs coeff (mm$^{-1}$) | 2.504 | 2.208 | 6.293 | 2.161 | 2.299 |
| cryst size (mm) | 0.15 × 0.15 × 0.04 | 0.50 × 0.30 × 0.15 | 0.48 × 0.30 × 0.05 | 0.50 × 0.30 × 0.25 | 0.34 × 0.34 × 0.09 |
| no. of unique data | 15 810 | 13 029 | 13 922 | 3473 | 3457 |
| no. of obsd data ($I > 2\sigma(I)$) | 10 449 | 10 536 | 12 367 | 3166 | 3326 |
| no. of variables | 823 | 1270 | 1251 | 298 | 298 |
| *R* indices ($I < 2\sigma(I)$) | R1[a] = 0.0683 | R1[a] = 0.0497 | R1[a] = 0.0445 | R1[a] = 0.0663 | R1[a] = 0.0305 |
| | wR2[b] = 0.1435 | wR2[b] = 0.1013 | wR2[b] = 0.1007 | wR2[b] = 0.1724 | wR2[b] = 0.0325 |
| *R* indices (all data) | R1[a] = 0.1172 | R1[a] = 0.0724 | R1[a] = 0.0552 | R1[a] = 0.0731 | R1[a] = 0.0325 |
| | wR2[b] = 0.1694 | wR2[b] = 0.1213 | wR2[b] = 0.1161 | wR2[b] = 0.1864 | wR2[b] = 0.0861 |

[a] $R1 = \sum||F_o| - |F_c||/\sum|F_o|$. [b] $wR2 = [\sum w(F_o^2 - F_c^2)^2/\sum(w|F_o|^2)^2]^{1/2}$.

**Table 3. Selected Bond Lengths (Å) and Angles (deg) for 1c**

| | | | |
|---|---|---|---|
| W−Co(1) | 2.7048(5) | Co(1)−C(1) | 1.935(4) |
| W−Co(2) | 2.6498(6) | Co(1)−C(11) | 1.792(6) |
| Co(1)−Co(2) | 2.4907(8) | Co(1)−C(12) | 1.793(5) |
| W−C(1) | 2.075(3) | Co(1)−C(13) | 1.781(6) |
| W−C(31) | 1.991(6) | Co(2)−C(1) | 1.922(4) |
| W−C(32) | 1.974(5) | Co(2)−C(21) | 1.810(5) |
| W−C(33) | 2.326(5) | Co(2)−C(22) | 1.806(5) |
| W−C(34) | 2.319(5) | Co(2)−C(23) | 1.790(5) |
| W−C(35) | 2.331(4) | C(1)−C(2) | 1.468(6) |
| W−C(36) | 2.362(5) | C(2)−O(1) | 1.192(6) |
| W−C(37) | 2.362(5) | C(2)−O(2) | 1.329(6) |
| Co(1)−W−Co(2) | 55.43(2) | W−Co(2)−Co(1) | 63.41(2) |
| C(1)−W−C(31) | 84.4(2) | C(1)−Co(2)−C(22) | 98.8(2) |
| C(1)−W−C(32) | 76.6(2) | C(1)−Co(2)−C(23) | 104.4(2) |
| C(1)−W−C(33) | 151.6(2) | C(21)−Co(2)−C(22) | 104.6(2) |
| C(1)−W−C(34) | 165.0(2) | C(21)−Co(2)−C(23) | 100.3(2) |
| C(1)−W−C(35) | 149.3(2) | C(22)−Co(2)−C(23) | 98.4(2) |
| C(1)−W−C(36) | 135.3(2) | W−C(1)−Co(1) | 84.7(1) |
| C(1)−W−C(37) | 136.4(2) | W−C(1)−Co(2) | 82.9(1) |
| W−Co(1)−Co(2) | 61.17(2) | W−C(1)−C(2) | 133.8(3) |
| C(1)−Co(1)−C(11) | 103.1(2) | Co(1)−C(1)−Co(2) | 80.4(2) |
| C(1)−Co(1)−C(12) | 102.0(2) | Co(1)−C(1)−C(2) | 125.7(3) |
| C(1)−Co(1)−C(13) | 141.2(2) | Co(2)−C(1)−C(2) | 130.9(3) |
| C(11)−Co(1)−C(12) | 96.9(2) | C(1)−C(2)−O(1) | 126.0(4) |
| C(11)−Co(1)−C(13) | 101.7(3) | C(1)−C(2)−O(2) | 111.9(4) |
| C(12)−Co(1)−C(13) | 104.1(2) | C(2)−O(2)−C(3) | 116.5(5) |
| C(1)−Co(2)−C(21) | 142.8(2) | O(1)−C(2)−O(2) | 122.1(4) |

yield on a sufficiently large scale to be useful. The cluster ligand precursor $(CO)_9Co_3(\mu_3\text{-CCOOH})$ can be simply prepared on multigram scales,[4,7,14,15] and metal fragment exchange is a well-established mode for cluster modification.[18] Thus, we examined the reaction of $[CpMo(CO)_3]_2$ with $(CO)_9Co_3(\mu_3\text{-CCOOH})$ as it is a known route to $CpMo(CO)_2Co_2(CO)_6(\mu_3\text{-CR})$ for a variey of organic R groups.[19] However, all attempts to carry out metal fragment exchange on the cluster acid led to extensive cluster degradation, and only traces of product could be observed.

A successful approach began by protecting the carboxylic acid group by esterification, i.e., $(CO)_9Co_3(\mu_3\text{-CC(O)OR})$ (R = $C_2H_5$ or $CH(CH_3)_2$) was used for the metal exchange reaction. To increase the efficiency, the protected compound was prepared directly from commerically available $Cl_3CC(O)OR$ and $Co_2(CO)_8$. The $CpM'(CO)_2$ (M′ = Mo, W) fragment exchange of the protected cluster cleanly yielded $CpM'(CO)_2Co_2(CO)_6(\mu_3\text{-CC(O)OR})$. De-esterification in concentrated $H_2SO_4$ followed by hydrolysis gave $CpM'(CO)_2Co_2(CO)_6(\mu_3\text{-CCOOH})$ (**1a** and **1b**) in good yield on a multigram scale. Presumably, $[CpM'(CO)_2Co_2(CO)_6(\mu_3\text{-CCO})]^+$ is formed and then hydrolyzed.[15]

**Chart 1**

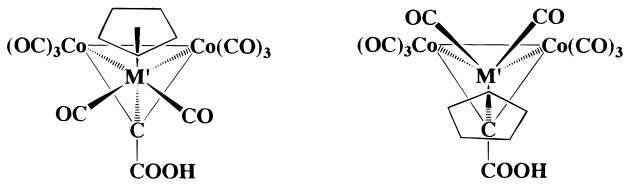


The $CpM'(CO)_2Co_2(CO)_6(\mu_3\text{-CR})$ cluster system has been well-studied in both the solid state and in solution, and considerable interest in the past in this cluster concerned the structural isomerism associated with the $CpM'(CO)_2$ fragment.[20−22] Two distinct rotamers, defined by the orientation of the $CpM'(CO)_2$ group relative to the remainder of the cluster, have been observed. Thus, for $\eta^5$-$C_5H_5$ and $\eta^5$-$C_5H_4Me$ derivatives, the cyclopentadienyl group is distal relative to the carbyne carbon (Chart 1a) in the solid state. For a $\eta^5$-$C_5Me_5$ derivative, the group is proximal in the solid state (Chart 1b). In the proximal isomer, the carbonyl ligands associated with the group 6 metal are semibridging, giving this species a characteristically different IR signature. Electronic factors associated with the properties of the $\eta^5$-$C_5R_5$ ligands, rather than steric effects, have been suggested as the origin of the observed

(18) *The Chemistry of Metal Cluster Complexes*; Shriver, D. F., Kaesz, H. D., Adams, R. D., Eds.; VCH: New York, 1990.

(19) Mlekuz, M.; Bougeard, P.; Sayer, B. G.; Faggiani, R.; Lock, C. J. L.; McGlinchey, M. J.; Jaouen, G. *Organometallics* **1985**, *4*, 2046.

(20) Chetcuti, M. J.; Chetcuti, P. A. M.; Jeffery, J. C.; Mills, R. M.; Mitrprachachon, P.; Pickering, S. J.; Stone, F. G. A.; Woodward, P. *J. Chem. Soc., Dalton Trans.* **1982**, 699.

(21) Beurich, H.; Vahrenkamp, H. *Angew. Chem., Int. Ed. Engl.* **1978**, *17*, 863.

(22) Sutin, K. A.; Li, L.; Frampton, C. S.; Sayer, B. G.; McGlinchey, M. J. *Organometallics* **1991**, *10*, 2362.

**Table 4. Selected Bond Lengths (Å) and Angles (deg) for 2·2THF[a]**

| | | | |
|---|---|---|---|
| Zr−Zr′ | 3.3987(13) | Co(11)−C(10) | 2.023(8) |
| Mo(11)−Co(11) | 2.6991(12) | Co(12)−C(10) | 1.910(7) |
| Mo(11)−Co(12) | 2.7667(12) | Mo(21)−C(20) | 2.070(7) |
| Co(11)−Co(12) | 2.700(2) | Co(21)−C(20) | 1.867(7) |
| Mo(21)−Co(22) | 2.6562(12) | Co(22)−C(20) | 1.958(8) |
| Mo(21)−Co(21) | 2.6789(12) | Mo(31)−C(30) | 1.970(7) |
| Co(21)−Co(22) | 2.715(2) | Co(31)−C(30) | 1.983(7) |
| Mo(31)−Co(32) | 2.5362(13) | Co(32)−C(30) | 2.018(8) |
| Mo(31)−Co(31) | 2.5864(13) | O(1)−Zr′ | 2.177(5) |
| Co(31)−Co(32) | 2.524(2) | C(10)−C(11) | 1.371(9) |
| Zr−O(1) | 2.066(5) | C(11)−O(11) | 1.309(8) |
| Zr−O(12) | 2.121(5) | C(11)−O(12) | 1.374(9) |
| Zr−O(22) | 2.158(5) | C(20)−C(21) | 1.433(10) |
| Zr−O(1)′ | 2.177(5) | C(21)−O(21) | 1.311(9) |
| Zr−O(11) | 2.253(5) | C(21)−O(22) | 1.368(9) |
| Zr−O(32) | 2.269(5) | C(30)−C(31) | 1.575(10) |
| Zr−O(31) | 2.292(5) | C(31)−O(32) | 1.273(8) |
| Zr−O(21) | 2.344(5) | C(31)−O(31)′ | 1.291(8) |
| Mo(11)−C(10) | 1.929(7) | | |
| O(1)−Zr−O(12) | 149.2(2) | C(10)−Co(12)−Co(11) | 48.4(2) |
| O(1)−Zr−O(22) | 110.2(2) | C(10)−Co(12)−Mo(11) | 44.2(2) |
| O(12)−Zr−O(22) | 80.3(2) | C(20)−Mo(21)−Co(22) | 47.0(2) |
| O(1)−Zr−O(1)′ | 73.6(2) | C(20)−Mo(21)−Co(21) | 44.0(2) |
| O(12)−Zr−O(1)′ | 111.5(2) | Co(22)−Mo(21)−Co(21) | 61.17(4) |
| O(22)−Zr−O(1)′ | 151.2(2) | C(20)−Co(21)−Mo(21) | 50.4(2) |
| O(1)−Zr−O(11) | 142.1(2) | C(20)−Co(21)−Co(22) | 46.2(2) |
| O(12)−Zr−O(11) | 65.6(2) | Mo(21)−Co(21)−Co(22) | 59.00(3) |
| O(22)−Zr−O(11) | 83.8(2) | C(20)−Co(22)−Mo(21) | 50.6(2) |
| O(1)′−Zr−O(11) | 78.1(2) | C(20)−Co(22)−Co(21) | 43.5(2) |
| O(1)−Zr−O(32) | 75.1(2) | Mo(21)−Co(22)−Co(21) | 59.83(4) |
| O(12)−Zr−O(32) | 75.9(2) | C(30)−Mo(31)−Co(32) | 51.4(2) |
| O(22)−Zr−O(32) | 127.9(2) | C(30)−Mo(31)−Co(31) | 49.3(2) |
| O(1)′−Zr−O(32) | 80.8(2) | Co(32)−Mo(31)−Co(31) | 59.02(4) |
| O(11)−Zr−O(32) | 124.6(2) | C(30)−Co(31)−Co(32) | 51.5(2) |
| O(1)−Zr−O(31) | 82.3(2) | C(30)−Co(31)−Mo(31) | 48.9(2) |
| O(12)−Zr−O(31) | 128.5(2) | C(337)−Co(31)−Mo(31) | 45.8(2) |
| O(22)−Zr−O(31) | 78.1(2) | Co(32)−Co(31)−Mo(31) | 59.50(4) |
| O(1)′−Zr−O(31) | 74.1(2) | C(30)−Co(32)−Mo(31) | 49.7(2) |
| O(11)−Zr−O(31) | 66.0(2) | Co(31)−Co(32)−Mo(31) | 61.48(4) |
| O(32)−Zr−O(31) | 150.1(2) | Zr−O(1)−Zr′ | 106.4(2) |
| O(1)−Zr−O(21) | 80.5(2) | Zr−O(1)−H(1) | 114(7) |
| O(12)−Zr−O(21) | 79.6(2) | Zr′−O(1)−H(1) | 131(7) |
| O(22)−Zr−O(21) | 61.9(2) | Mo(11)−C(10)−Co(11) | 86.1(3) |
| O(1)′−Zr−O(21) | 144.1(2) | O(11)−C(11)−C(10) | 114.8(7) |
| O(11)−Zr−O(21) | 134.9(2) | O(11)−C(11)−O(12) | 124.4(6) |
| O(32)−Zr−O(21) | 68.6(2) | C(10)−C(11)−O(12) | 120.7(6) |
| O(31)−Zr−O(21) | 126.8(2) | C(11)−O(11)−Zr | 83.0(4) |
| C(10)−Mo(11)−Co(11) | 48.4(2) | C(11)−O(12)−Zr | 86.9(4) |
| C(10)−Mo(11)−Co(12) | 43.6(2) | C(21)−C(20)−Co(21) | 119.5(5) |
| Co(11)−Mo(11)−Co(12) | 59.19(4) | C(21)−C(20)−Co(22) | 131.5(6) |
| C(10)−Co(11)−Mo(11) | 45.5(2) | Co(21)−C(20)−Co(22) | 90.4(3) |
| C(10)−Co(11)−Co(12) | 44.9(2) | C(21)−C(20)−Mo(21) | 132.8(5) |
| Mo(11)−Co(11)−Co(12) | 61.65(4) | Co(21)−C(20)−Mo(21) | 85.6(3) |
| Co(22)−C(20)−Mo(21) | 82.4(3) | O(32)−C(31)−O(31)′ | 120.1(6) |
| O(21)−C(21)−O(22) | 120.1(6) | O(32)−C(31)−C(30) | 118.8(6) |
| O(21)−C(21)−C(20) | 116.5(7) | O(31)′−C(31)−C(30) | 121.0(6) |
| O(22)−C(21)−C(20) | 123.5(7) | C(31)′−O(31)−Zr | 133.6(4) |
| C(21)−O(21)−Zr | 85.7(4) | C(31)−O(32)−Zr | 135.0(4) |
| C(21)−O(22)−Zr | 92.2(4) | O(136)−C(136)−Mo(11) | 176.1(7) |
| C(31)−C(30)−Mo(31) | 134.2(5) | O(137)−C(137)−Mo(11) | 173.4(8) |
| C(31)−C(30)−Co(31) | 135.2(5) | O(236)−C(236)−Mo(21) | 173.1(8) |
| Mo(31)−C(30)−Co(31) | 81.7(3) | O(237)−C(237)−Mo(21) | 173.2(7) |
| C(31)−C(30)−Co(32) | 126.8(5) | O(336)−C(336)−Mo(31) | 174.0(7) |
| Mo(31)−C(30)−Co(32) | 79.0(3) | O(337)−C(337)−Mo(31) | 172.1(7) |
| Co(31)−C(30)−Co(32) | 78.2(3) | | |

[a] Symmetry transformation used to generate equivalent atoms: $-x + 1, -y + 1, -z + 1$.



effect.[22] The difference in energy between the two isomeric forms is small as both are present in solution; however, the predominant isomer is the one found in the solid state for the cyclopentadienyl derivative in question.

As described below, the solid state structures reveal that it is exclusively the proximal isomer of the cluster ligand that is bound to Ti(IV) or Zr(IV). In order to interpret the solution behavior of the coordinated cluster, it is necessary to discuss the spectroscopic behavior and acidity of cluster acids **1**. First, the solid state structure of $CpW(CO)_2Co_2(CO)_6(\mu_3\text{-}CC(O)OC_2H_5)$ establishes the distal isomer as the most stable form in the solid state for the ester, as expected (Figure 1). For this species, a comparison of the solid state and solution IR spectra clearly shows that some proximal isomer is present in solution. Not only are bridging carbonyl bands present in solution, but most of the terminal

**Table 5. Selected Average Bond Lengths (Å) and Angles (deg) for 3a·$CH_2Cl_2$, 3b·$CH_2Cl_2$, 3c, and 3d**

| | 3a | 3b | 3c·$CH_2Cl_2$ | 3d·$CH_2Cl_2$ |
|---|---|---|---|---|
| | | Distances (Å) | | |
| M−Co | 2.731(5) | 2.737 (8) | 2.731(3) | 2.736(5) |
| Co−Co | 2.517(7) | 2.494(13) | 2.520(3) | 2.510(2) |
| Ti···Ti | 2.915(7) | 2.912(3) | 2.945(4) | 2.906(3) |
| | 3.031(3) | 3.033(3) | 3.038(3) | 3.032(3) |
| Ti−$\mu_3$-O | 1.920(11) | 1.920(10) | 1.921(1) | 1.919(1) |
| | 2.104(7) | 2.106(7) | 2.105(7) | 2.106(6) |
| Ti−$O_c$[a] | 2.034(10) | 2.033(11) | 2.026(3) | 2.027(4) |
| Ti−OR | 1.762(7) | 1.82(9) | 1.792(9) | 1.771(6) |
| $O_c$−C | 1.27(2) | 1.27(1) | 1.28(1) | 1.27(3) |
| | | Angles (deg) | | |
| Co−M−Co | 54.9(2) | 54.2(3) | 54.95(6) | 54.61(4) |
| M−Co−Co | 62.6(2) | 62.9(4) | 62.53(1) | 62.7(2) |
| $\mu_3$-O−Ti−$\mu_3$-O | 81.4(6) | 81.4(5) | 80.6(8) | 81.5(3) |
| $\mu_3$-O−Ti−OR | 104(2) | 103(2) | 102(2) | 103(2) |
| | 172.3(7) | 172.5(3) | 174.4(4) | 173.1(3) |
| $\mu_3$-O−Ti−$O_c$ | 89(2) | 89(2) | 90(2) | 90(3) |
| | 161.9(4) | 161.8(3) | 162.1(3) | 161.8(5) |
| | 82(1) | 82(1) | 83(1) | 82(2) |
| $O_c$−Ti−$O_c$ | 96.4(3) | 96.6(6) | 97.2(3) | 96.9(2) |
| Ti−O−R | 152(2) | 153(2) | 155(2) | 156(1) |
| Ti−$O_c$−C | 128.2(8) | 129.0(7) | 127.5(2) | 128(1) |
| $O_c$−C−$O_c$ | 124(1) | 123(1) | 124.6(10) | 123.0(8) |
| $O_c$−C−C | 118(2) | 119(1) | 118(1) | 118(2) |

[a] $O_c$ = oxygen atom of the cluster carboxylate.

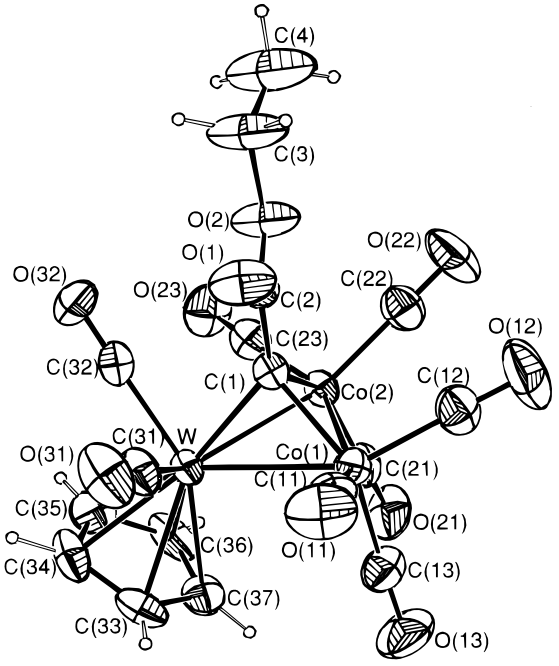


**Figure 1.** ORTEP plot of $CpW(CO)_2Co_2(CO)_6(\mu_3\text{-}CCO_2C_2H_5)$, **1c**, with thermal ellipsoids at 40% probability. The hydrogen atoms are drawn with an arbitrary radius for clarity.

carbonyl bands are doubled. Specifically, this permits the distinctive CO stretch at 2080 $cm^{-1}$ to be assigned to the distal isomer and that at 2090 $cm^{-1}$ to the proximal isomer. Although solid state structures are not available for the cluster acids **1a** and **1b**, the IR spectra in the solid state vs solution show similar distinctive differences and permit the same assignments.

We have previously argued that $[(CO)_9Co_3(\mu_3\text{-}CCO_2)]^-$ is a better ligand than $[CH_3CO_2]^-$ based on a correlation of measured Brönsted acidities and ligand displacement reactions.[4] Given the known electronic effects of CO vs Cp ligands, it is reasonable that the group 6 metal derivatives will be even weaker acids and, therefore, will constitute even more strongly bound ligands. Consistent with this hypothesis, the solid state IR spectra of **1a** and **1b** show that stretching frequencies of the $-CO_2H$ group (1632 and 1630 $cm^{-1}$, respectively) are at lower frequencies than those of $(CO)_9Co_3(\mu_3\text{-}CCOOH)$ (1640 $cm^{-1}$) which, in turn are lower than those of organic acids (1720−1706 $cm^{-1}$). The same holds in solution, although both monomer and dimer are now present (**1a**, 1678, 1632 $cm^{-1}$; **1b**, 1679, 1632 $cm^{-1}$; $(CO)_9Co_3(\mu_3\text{-}CCOOH)$, 1686, 1642 $cm^{-1}$). Thus, the predicted order of ligand binding strength for $[RCO_2]^-$ is R = $CH_3$ < $(CO)_9Co_3(\mu_3\text{-}C-)$ < $CpW(CO)_2Co_2(CO)_6(\mu_3\text{-}C-)$.

In order to compare ligand sizes, we have calculated the molecular volumes of each cluster ligand using experimentally obtained geometries. $CpM'(CO)_2Co_2(CO)_6(\mu_3\text{-}C-)$ is found to have a volume ca. 20% larger than that of $(CO)_9Co_3(\mu_3\text{-}C-)$, and the distal and proximal isomers of $CpM'(CO)_2Co_2(CO)_6(\mu_3\text{-}C-)$ have approximately the same volume. Thus, it is reasonable to expect that the observed differences in the chemistry between tricobalt and these mixed-metal cluster ligands will be due, principally, to differences in electronic rather than steric factors.

**Cluster-Substituted Group 6 Complexes. $Zr_2(\mu\text{-}OH)_2\{\mu\text{-}CpMo(CO)_2Co_2(CO)_6(\mu_3\text{-}CCO_2)\}_2\{\eta^2\text{-}CpMo(CO)_2Co_2(CO)_6(\mu_3\text{-}CCO_2)\}_4$, 2.** Compound **2** was obtained in good yield by the direct reaction of $[Zr(OCH(CH_3)_2)_4\cdot HOCH(CH_3)_2]_2$ with the cluster acid **1a** in THF. The solid state IR shows the characteristic stretching frequencies for carbonyl groups and carboxylato groups but, in contrast to all previous complexes of this type, none corresponding to alkoxy groups were present. The X-ray structure shows that all of the isopropoxide groups of the starting material have reacted with the cluster acid to yield the centrosymmetric dimer $[Zr_2(OH)_2\{Cp(CO)_2Mo(CO)_6Co_2(\mu_3\text{-}CCO_2)\}_6]$, **2** (Figure 2). There are two bridging cluster ligands, four chelating cluster ligands, and two bridging hydroxo groups generating a $Zr_2O_{14}$ core and a coordination number of eight for each Zr atom. Consistent with the complexity of the carboxylate region of the IR, symmetrical bridging (Zr−O = 2.269(5) vs 2.292(5) Å) and unsymmetrical chelating (Zr−O = 2.121(5), 2.158(5) Å vs 2.253(5), 2.344(5) Å) bonding modes are observed for the cluster ligands. The hydroxo bridges are unsymmetrical (2.066(5), 2.177(5) Å). A weak band at 3110 $cm^{-1}$ in the IR is assigned to the OH. The coordination geometry of each Zr atom can be described as a distorted dodecahedron with two oxygen atoms from hydroxo ligands, two from bridging carboxylates, and four from chelating carboxylates. This leads to an edge-shared bidodecahedral $Zr_2O_{14}$ core structure. The Zr−Zr distance is similar to that observed in $[Zr_2(OCH(CH_3)_2)_4\{(CO)_9Co_3(\mu_3\text{-}CCO_2)\}_4]$.

The Cp rings of the $CpMo(CO)_2$ moieties in **2** are proximal rather than distal with respect to the carbyne capping units. The molybdenum carbonyls become semibridging (Mo−C−O angles from 172.1(7)° to 176.1(7)°) to their neighboring cobalt atoms, consistent with the presence of the band at 1894 $cm^{-1}$ in the solid state IR spectrum.

**$Ti_4(\mu_3\text{-}O)_4(OR)_4\{\mu\text{-}CpM'(CO)_2Co_2(CO)_6(\mu_3\text{-}CCO_2)\}_4$ (R = $CH(CH_3)_2$, M′ = Mo (3a), W (3b); R = $CH_2CH_3$, M′ = Mo (3c), W (3d).** Prepared from the

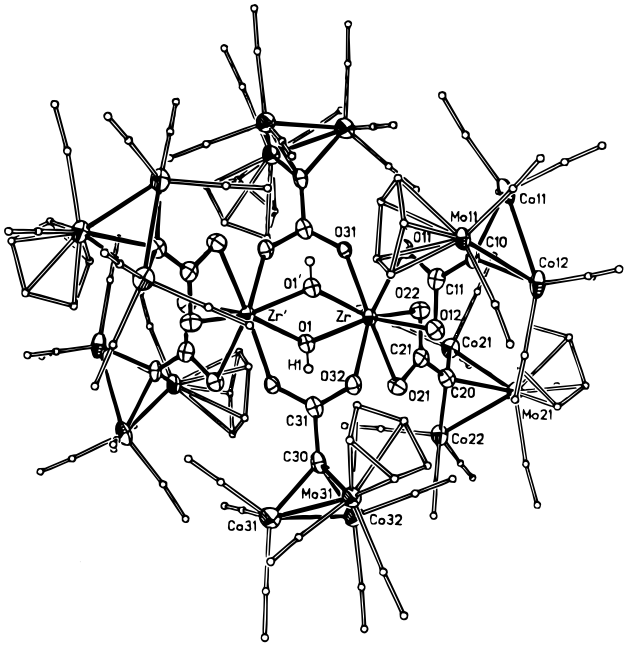


**Figure 2.** ORTEP plot of $Zr_2(\mu\text{-}OH)_2\{\mu\text{-}CpMo(CO)_2Co_2(CO)_6(\mu_3\text{-}CCO_2)\}_2\{\eta^2\text{-}CpMo(CO)_2Co_2(CO)_6(\mu_3\text{-}CCO_2)\}_4$, **2**, with thermal ellipsoids at 40% probability. The carbon atoms of the Cp groups and the carbon and oxygen atoms of the carbonyl groups are drawn at arbitrary radii, and the hydrogen atoms of the Cp rings are omitted for clarity.

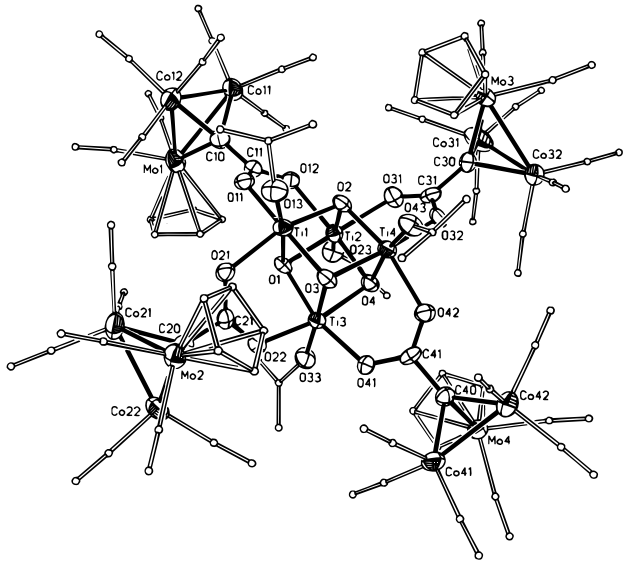


**Figure 3.** ORTEP plot of $Ti_4(\mu_3\text{-}O)_4(OCH(CH_3)_2)_4\{\mu\text{-}CpMo(CO)_2Co_2(CO)_6(\mu_3\text{-}CCO_2)\}_4$, **3a**, with thermal ellipsoids at 40% probability. The carbon atoms of the Cp groups and the carbon and oxygen atoms of the carbonyl groups are drawn at arbitrary radii, and the hydrogen atoms of the Cp rings are omitted for clarity.

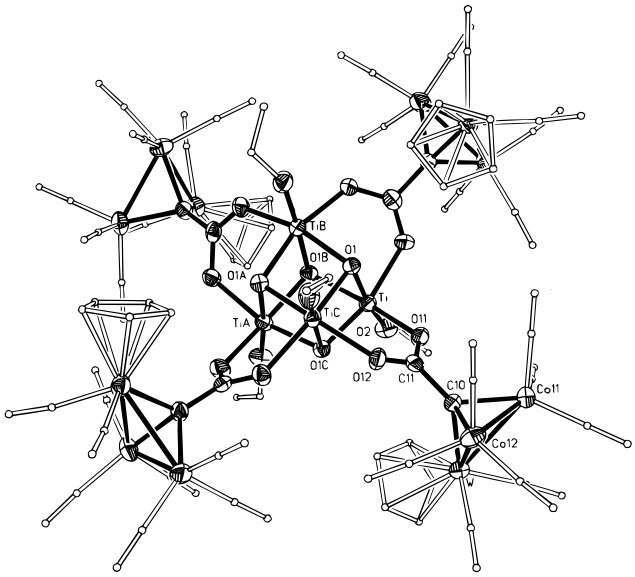


**Figure 4.** ORTEP plot of $Ti_4(\mu_3\text{-}O)_4(OCH_2CH_3)_4\{\mu\text{-}CpW(CO)_2Co_2(CO)_6(\mu_3\text{-}CCO_2)\}_4$, **3d**, with thermal ellipsoids at 40% probability. The carbon atoms of the Cp groups and the carbon and oxygen atoms of the carbonyl groups are drawn at arbitrary radii, and the hydrogen atoms of the Cp rings are omitted for clarity.

reaction of titanium alkoxides and the cluster acids, compounds **3** possess solid state IR spectra that exhibit bands characteristic of terminal carbonyls, semibridging carbonyls, bridging carboxylates, and alkoxides. The $^1H$ NMR spectra refect the presence of the Cp and alkoxide moieties. Comparison of the solution and solid state IR spectra confirm that the compounds remain intact in solution.

The solid state structural studies show that **3a** and **3b** are isostructural, as are **3c** and **3d**. Figures 3 and 4 show the molecular structures of **3a** and **3d**, respectively, and all have virtual $S_4$ symmetry (**3a** and **3b** lie in general positions, whereas **3c** and **3d** lie on crystallographic $S_4$ axes). The core consists of a distorted $Ti_4O_4$ cube with Ti(IV) and $\mu_3$-O occupying alternate vertices. Each Ti(IV) lies in the center of a distorted octahedron of O atoms with three derived from bridging oxo ligands, two from bridging cluster ligands, and one from a terminal alkoxide ligand. The cluster carboxylates bridge four of the six edges of the $Ti_4$ tetrahedron, and the four bridged carboxylates form a butterfly shape such that an $S_4$ axis runs through the centers of the two unbridged edges. Thus, the four trimetal clusters lie roughly in a plane perpendicular to the $S_4$ axis with one transoid pair being displaced slightly up and one pair down. The R groups of the alkoxy ligands as well as the Cp groups of the clusters project above and below the plane of the clusters. In **3**, the Cp rings of the $CpM'(CO)_2$ moieties are proximal with respect to the carbyne capping units and the $CpM'(CO)_2$ carbonyls are semibridging, just as found for **2**. This is consistent with the bands observed in the solid state IR.

**Significance of the Isomeric Form of the Bound Cluster Ligand.** In contrast to the cluster ligands where the solution IR showed the presence of both isomers, the IR spectra of **2** and **3** in the two phases are nearly the same, e.g., for **3a** a band is observed at 2087 $cm^{-1}$ in solution and the solid state corresponding to the proximal isomer, but no band is observed at ca. 2080 $cm^{-1}$ for the distal isomer. Clearly, only the proximal isomer binds, and no isomerization to the distal form is observed in solution. The progressive disappearance of the distal isomer during the synthesis of **2** is illustrated in Figure 5. The exclusive coordination of the proximal form causes a shift in the distal−proximal solution equilibrium and a continuous loss of intensity in the bands associated with the distal form (e.g., 2080 $cm^{-1}$). The IR results are confirmed by the solution $^{13}C$ NMR of **3c** (see also below) which exhibits a Cp chemical shift characteristic of the proximal isomer ($\delta$ 94) and none for the distal isomer ($\delta$ 90).[22]

**Chart 2**

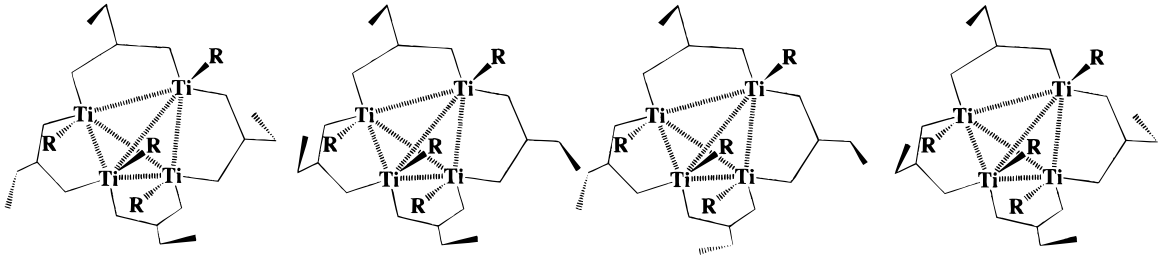


**(a) $S_4$, 4 eq Cp, 4 eq R** **(b) $C_{2v}$, 4 eq Cp, 2 pr eq R** **(c) $C_s$, 2 pr eq Cp, 1 pr eq R + 2 R** **(d) $C_1$, 4 Cp, 4 R**

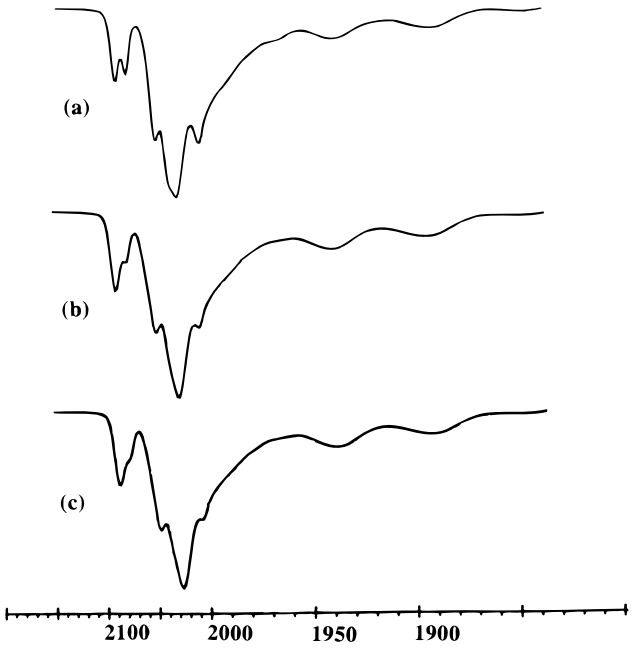


**Figure 5.** Solution IR in THF (2200−1800 $cm^{-1}$ ): (a) $CpMo(CO)_2Co_2(CO)_6(\mu_3\text{-}CCOOH)$, **1a**; (b) After reaction of **1a** and $[Zr(OCH(CH_3)_2\cdot HOCH(CH_3)_2]_2$ at 50 °C for 1 h; (c) After reaction at 50 °C for 24 h.

Although there is no question that the proximal isomer is the only form of the bound cluster, the $^1H$ NMR spectra of **3a**−**d**, but not that of **2**, show that in solution more than a single structural form is present. Thus, for the isopropyl derivatives, **3a** and **3b**, two types of Cp and $CH_3$ signals are observed in about a 1:5 ratio. For the ethyl derivatives, **3a** and **3b**, the results for **3b** given in parentheses, the situation is even more complex in that four (six) types of Cp, two (two) types of $CH_2$, and three (four) types of $CH_3$ groups can be discerned. For **3a**, the Cp resonance in the 126 MHz $^{13}C$ NMR shows a complexity of signals and a pattern much like that observed for the Cp protons in the $^1H$ NMR. In both cases, a small chemical shift range is observed (0.028 ppm for $^1H$ and 0.08 ppm for $^{13}C$, see Experimental Section). Clearly, isomeric forms of the cluster coordination compound are being observed, and the number of these isomers depends on the size of the alkoxy ligand.

We suggest that these isomers arise from the loss of free rotation of the $Co_2M'$ metal triangle, that is the alkylidyne cluster, around the $\mu_3$-C−C($CO_2^-$) bond axis after coordination of the ligand. The fact that the number of isomers observed increases as the size of the alkyl group decreases provides key support for this hypothesis. A significant barrier may exist because the cluster cone angle of a $CpM(CO)_2$ fragment is significantly larger than that of a $M(CO)_3$ fragment.[23] In order to rotate the metal triangle around the C−C axis, this large metal fragment must pass by the alkyl group of the alkoxy ligand (Figures 3 and 4). In addition, in the proximal form, the bulkier part of the $CpM(CO)_2$ fragment is placed even closer to the carboxylate moiety (and the alkyl group of RO). If free rotation around the capping $\mu_3$-C−C bond axis is restricted, then there four ways of arranging the cluster ligands around the $Ti_4O_4$ core, as shown schematically in Chart 2. In this chart, the relative orientations of the Cp moieties with respect to the R groups and the $Ti_4$ tetrahedron are shown. The "flags" point to the side of the plane defined by the $-CO_2^-$ where the Cp moiety lies. The number of different Cp and R groups are given for each isomeric form. As seen in Chart 2, the total number of types of Cp and R groups possible is 8 and 10, respectively. The four forms will have different stabilities, and as the difference in stabilities will depend on the size of the alkyl group, the number of Cp and R groups observed will differ for the ethyl vs isopropyl derivatives. However, assignment of specific signals to specific forms is not possible. The variable-temperature $^1H$ NMR (22−50 °C) was carried out, but only minor changes in peak width, chemical shifts, and peak intensities were observed. Note that the existence of the isomeric forms shown in Chart 2 would not have a measurable effect on the carbonyl bands in the IR as the internal M−CO interactions are unchanged by rotation about the $\mu_3$-C−C bond axis.

The fact that the proximal isomer is found exclusively in the carboxylate products provides independent evidence that a cluster electronic effect is the driving force for this chemistry. As noted above, there is good spectroscopic evidence that carboxylate $[RCO_2]^-$ binding increases in the order R = $CH_3$ < $(CO)_9Co_3(\mu_3\text{-}C-)$ < $CpW(CO)_2Co_2(CO)_6(\mu_3\text{-}C-)$. It has been suggested that the proximal orientation of the $CpM(CO)_2$ fragment leads to significant electronic donation to the other two metal centers and, presumably, to the capping functional group.[22] Thus, as observed, the proximal isomer is a better ligand than the distal isomer.

**Cluster Substituent Effects.** The outcome of the reactions of **1** with Ti and Zr alkoxides are compared with the corresponding reactions observed with the tricobalt cluster ligand in Chart 3. Although the predominant product structure type is the tetrameric cubane **3**, there are some significance differences be-

(23) Mingos, D. M. P. *Inorg. Chem.* **1982**, *21*, 464.

**Chart 3**

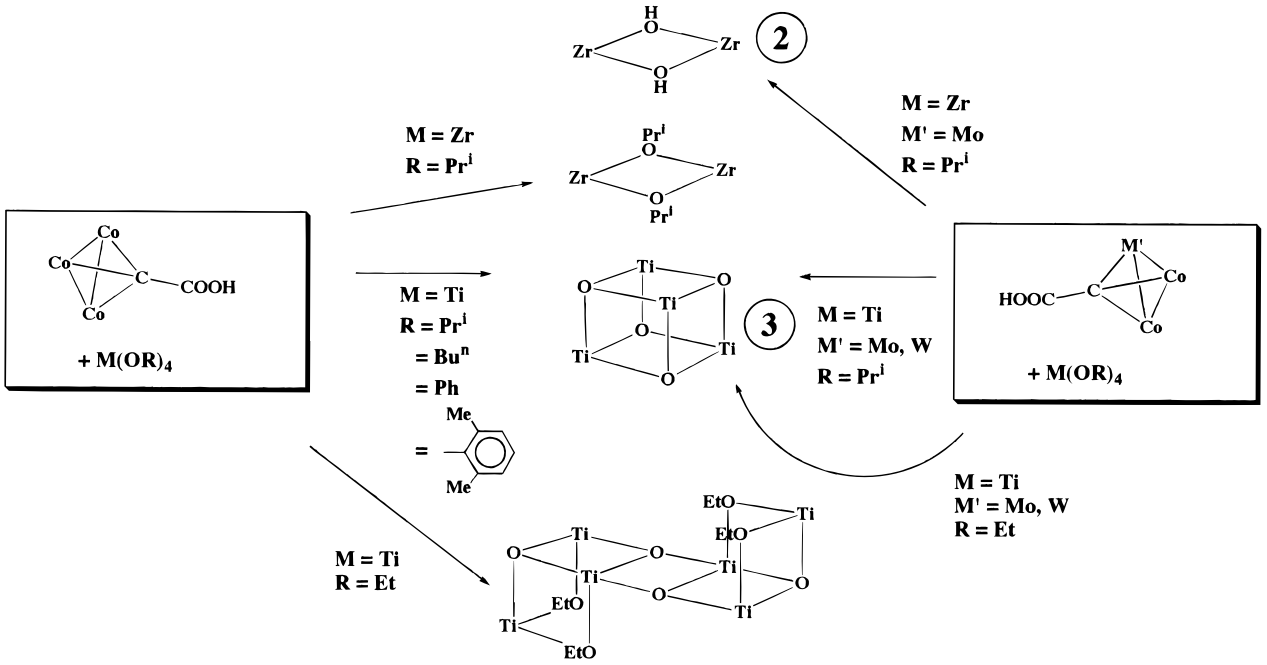


**Chart 4**

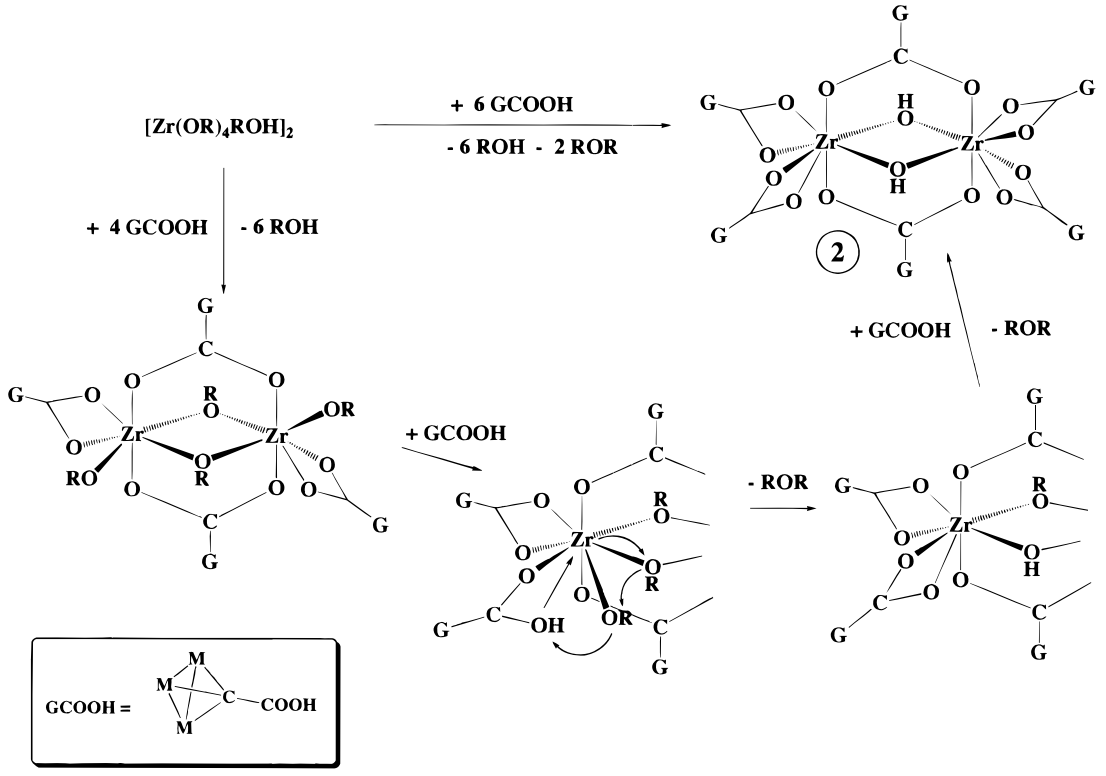


tween the two systems. For Zr, a dimeric product is observed for both cluster ligands, i.e., **2** for the modified cluster ligand **1** and $Zr_2(\mu\text{-}OCH(CH_3)_3)_2(OCH(CH_3)_3)_2\text{-}\{(CO)_3Co_3(\mu_3\text{-}CCO_2)\}_4$, **2′**, for the tricobalt cluster ligand. However, the use of **1** results in more extensive reaction in that complex **2** contains six cluster ligands rather than four, bridging OH groups rather than OR, and no alkoxide ligands at all.

The overall reaction for the formation of **2** is shown at the top of Chart 4. The formation of diisopropyl ether as a coproduct was confirmed by observing the IR of the volatile fraction taken from the reaction mixture. On the basis of the observations for the two different cluster ligands, the pathway for the formation of **2**, shown at the bottom of Chart 4, is postulated. The similarity of the chemistry observed for the reactions of **1** with Ti alkoxides (see below) suggests that the first product is one that has the composition and structure of **2′**. The subsequent steps are less certain but are consistent with the structure of the final product **2**. The Zr(IV) centers of **2** are now eight-coordinate vs seven-coordinate for **2′**, i.e., protonolysis of four RO ligands from the Zr dimer and displacement of two coordinated ROH. The two cluster ligands are of similar size, so this is additional evidence for the greater ligating ability of **1** vs the tricobalt cluster ligand (see above). Thus, we propose

an intermediate in which a molecule of the free cluster acid coordinates to one Zr center. This species leads easily to an OH-bridged species by ROR elimination, which may be facilitated by proton transfer from the coordinated acid.

In the case of Ti, reaction of the modified cluster acid with $Ti(OCH(CH_3)_2)_4$ leads to the same product stoichiometry and structure type **3** as formed from the tricobalt cluster. This is true both for the Mo and W derivatives of **1**. Presumably, they are formed by the pathway suggested in the preceding paper.[12] Alkoxides larger than isopropoxide did not change the outcome of the reaction for the tricobalt cluster ligand, but smaller $Ti(OCH_2CH_3)_4$ led to a hexameric product (Chart 1). In contrast, reaction of both the Mo and W derivatives of **1** with $Ti(OCH_2CH_3)_4$ lead to the same stoichiometry and structure as the isoproxide, i.e., the cubane **3**.

In the case of the tricobalt cluster ligand, we attributed the hexameric product to condensation of two trimers containing two cluster ligands each, i.e., $\{Ti(OCH_2CH_3)_4\}_3$ adds two cluster ligands with dimerization occurring more rapidly that the addition of a third cluster ligand. For the isoproxide and all other momomeric $Ti(OR)_4$, we suggested that the cubane tetramers result from condensation of $Ti(OR)_3\{(CO)_3Co_3(\mu_3\text{-}CCO_2)\}$ intermediates via $Ti_2(\mu\text{-}OR)_2(OR)_4\{(CO)_3Co_3(\mu_3\text{-}CCO_2)\}_2$ modeled by **2′**. Consistent with these hypotheses, we suggest that the even greater coordination power of **1** leads rapidly to a $Ti(OCH_2CH_3)_3\{CpM'(CO)_2(CO)_6Co_2(\mu_3\text{-}CCO_2)\}$ monomer which in turn gives the observed cubane tetramer. Note that the difference cannot be due to steric effects as the cluster ligands are nearly the same size.

**Acknowledgment.** We thank John Morelli for access to the program for calculating molecular volumes, Prof. A. G. Lappin for advice, Mr. D. Schifferl and Dr. J. Zajicek for aid with the NMR experiments, the National Science Foundation for funding, and the Department of Chemistry and Biochemistry for a Reilly Fellowship for X.L.

**Supporting Information Available:** Tables of crystal and refinement data, atomic coordinates, thermal parameters, atomic distances and angles, and least-squares planes (103 pages). Ordering information is given on any current masthead page.

OM9708384